



## RESEARCH ARTICLE

10.1002/2014WR015703

### Key Points:

- Drought Management Index (DMI) quantifies the drought propensity
- Spatiotemporal variation of DMI helps in adapting management policies
- Predictive potential of DMI can be used to assess the future drought propensity

### Correspondence to:

R. Maity,  
rajib@civil.iitkgp.ernet.in

### Citation:

Chanda, K., R. Maity, A. Sharma, and R. Mehrotra (2014), Spatiotemporal variation of long-term drought propensity through reliability-resilience-vulnerability based Drought Management Index, *Water Resour. Res.*, 50, doi:10.1002/2014WR015703.

Received 12 APR 2014

Accepted 4 SEP 2014

Accepted article online 8 SEP 2014

# Spatiotemporal variation of long-term drought propensity through reliability-resilience-vulnerability based Drought Management Index

Kironmala Chanda<sup>1</sup>, Rajib Maity<sup>1</sup>, Ashish Sharma<sup>2</sup>, and Rajeshwar Mehrotra<sup>2</sup>

<sup>1</sup>Department of Civil Engineering, Indian Institute of Technology Kharagpur, Kharagpur, West Bengal, India, <sup>2</sup>School of Civil and Environmental Engineering, University of New South Wales, Sydney, New South Wales, Australia

**Abstract** This paper characterizes the long-term, spatiotemporal variation of drought propensity through a newly proposed, namely Drought Management Index (DMI), and explores its predictability in order to assess the future drought propensity and adapt drought management policies for a location. The DMI was developed using the reliability-resilience-vulnerability (RRV) rationale commonly used in water resources systems analysis, under the assumption that depletion of soil moisture across a vertical soil column is equivalent to the operation of a water supply reservoir, and that drought should be managed not simply using a measure of system reliability, but should also take into account the readiness of the system to bounce back from drought to a normal state. Considering India as a test bed, 5 year long monthly gridded (0.5° Lat × 0.5° Lon) soil moisture data are used to compute the RRV at each grid location falling within the study domain. The Permanent Wilting Point (PWP) is used as the threshold, indicative of transition into water stress. The association between resilience and vulnerability is then characterized through their joint probability distribution ascertained using Plackett copula models for four broad soil types across India. The joint cumulative distribution functions (CDF) of resilience and vulnerability form the basis for estimating the DMI as a five-yearly time series at each grid location assessed. The status of DMI over the past 50 years indicate that drought propensity is consistently low toward northern and north eastern parts of India but higher in the western part of peninsular India. Based on the observed past behavior of DMI series on a climatological time scale, a DMI prediction model comprising deterministic and stochastic components is developed. The predictability of DMI for a lead time of 5 years is found to vary across India, with a Pearson correlation coefficient between observed and predicted DMI above 0.6 over most of the study area, indicating a reasonably good potential for drought management in the medium term water resources planning horizon.

## 1. Introduction

Droughts are periods marked by sustained water scarcity. They are known to produce adverse effects on agriculture, industry, and various other aspects of community life. Since droughts are *creeping* in nature, their onset is often difficult to identify [Sivakumar and Wilhite, 2002; Panu and Sharma, 2002]. As a result, drought management agencies may find it difficult to take necessary actions till the community is already reeling under severe water stress. Thus, drought management is as critical as it is challenging. Over the past century, numerous indices have been developed for the purpose of quantifying drought. The indices generally fall into three categories based on the type of drought quantified. Meteorological drought indices are used for measuring drought caused due to insufficient precipitation, agricultural drought indices quantify drought caused due to inadequate soil moisture while hydrological drought indices measure drought resulting from depletion of surface and sub surface water sources. Some of the widely used meteorological drought indices are Munger's Index [Munger, 1916], Precipitation Effectiveness Index [Thornthwaite, 1931], Blumenstock's Index [Blumenstock, 1942], Antecedent Precipitation Index (API) [McQuigg, 1954; Waggoner and O'Connell, 1956], Palmer Drought Severity Index (PDSI) [Palmer, 1965], Rainfall Anomaly Index (RAI) [van Rooy, 1965], Drought Area Index [Bhalme and Mooley, 1980], Standardized Precipitation Index (SPI) [McKee et al., 1993], and Effective precipitation [Byun and Wilhite, 1999]. Out of these, SPI is the most popular and easily computable. In its computation, precipitation is standardized so that it can be compared across time and space. Using the same methodology as SPI, Standardized Soil Moisture Index (SSMI) and Standardized

Streamflow Index (SSFI) [Modarres, 2007; Kao and Govindaraju, 2010] may be computed using soil moisture and streamflow respectively as the key variable, to serve as agricultural and hydrological drought indices, respectively. Among the other agricultural drought indices, Moisture Adequacy Index (MAI) [McGuire and Palmer, 1957], Moisture Anomaly Index (PMAI) (aka Z Index) [Palmer, 1965], Crop Moisture Index (CMI) [Palmer, 1968], Soil Moisture Anomaly Index (SMAI) [Bergman et al., 1988], Vegetation Condition Index (VCI) [Kogan, 1995; Liu and Kogan, 1996; Kogan, 1997], Computed Soil Moisture (CSM) [Huang et al., 1996] are the most important ones. Notable hydrological drought indices are Palmer Hydrological Drought Index (PHDI) [Palmer, 1965], Total Water Deficit (TWD) [Dracup et al., 1980], Surface Water Supply Index (SWSI) [Shafer and Dezman, 1982], and Cumulative Streamflow Anomaly (CSA) [Keyantash and Dracup, 2002]. A detailed comparison of these indices may be found in the analyses by Keyantash and Dracup [2002] and Heim [2002]. Most of the existing drought indices make use of a single metric in quantifying drought. Moreover, they are aimed at characterizing ongoing status of drought on a short time scale and therefore, are not well suited for analyzing droughts on a longer temporal scale. For example, in SPI calculation, the accumulated precipitation totals over the specified temporal scale are assumed to be independent. As a result, the effectiveness of SPI reduces with increase in temporal scale since the input precipitation series is not independent at such scales. Additionally, although SPI can be used to compare the drought severities at a certain point in time at different locations, it cannot be used to identify the drought prone areas [Mallya et al., 2013].

Hashimoto et al. [1982] demonstrated that reservoir system reliability, resilience, and vulnerability (RRV), which are established measures of system performance, may be effectively used for analysis of water resources system. With the assumption that depletion of soil moisture across a vertical soil column is equivalent to the operation of a water supply reservoir, the Drought Management Index (DMI) is derived using the RRV rationale [Maity et al., 2013]. Thus, by design, the DMI is a probabilistic drought index for characterizing droughts that differs from other indices in that it accounts for the readiness of a system to be able to bounce back from the drought, a factor that has till date not been taken into consideration in formulating drought relief or management plans. The soil stress level (e.g., Permanent Wilting Point [PWP]) is used as a threshold, indicative of transition into water stress. Since the water storage properties differ considerably across soil types, relationships between RRV, which are the properties of soil moisture series, are also expected to be distinct for each soil type. This issue can be addressed by determining individual dependence parameters for each soil type.

As is evident from the discussions in the previous paragraphs, existing drought indices are not ideally suited for assessing the slowly varying changes in drought propensity and do not consider the flexibility of the system to bounce back from drought to a normal state. Hence, in this study, the DMI is employed to assess the long-term, spatiotemporal variation of drought propensity over a large area with wide variation of climatic features. Moreover, the utility of DMI in distinguishing between regions with similar soil moisture reliability is explored. Finally, the challenge of predicting existing drought indices [Yuan and Wood, 2013] serves as motivation to explore the predictive potential of DMI which can indicate future drought propensities and help in adapting drought management policies for a location.

## 2. Methodology

The objectives of this paper are attained through the following broad steps (i) Computation of RRV of gridded monthly soil moisture data over the study area, (ii) Obtaining the joint probability distribution of resilience and vulnerability, specific to soil type, and (iii) Computation of DMI at each grid location over the study area. These are discussed in the following subsections.

### 2.1. Computation of Reliability-Resilience-Vulnerability (RRV)

Reliability, resilience, and vulnerability are three important measures of system performance. The concept of RRV in the context of water resources systems was established by Hashimoto et al. [1982] and was successfully applied for reservoir system analysis. When a reservoir system fulfils the demand for which it is designed, it is said to be *satisfactory* state, otherwise the system is said to be in *failure* state.

*Reliability* ( $x$ ) is defined by the probability that a system is in satisfactory state [Hashimoto et al., 1982]. It is given by

$$\alpha = P[X_t \in S] \tag{1}$$

where  $S$  represents satisfactory state.

As risk ( $\beta$ ) is the probability of a system being in failure state, it is given by

$$\beta = 1 - \alpha \tag{2}$$

For a given series, reliability is computed as

$$\alpha = \lim_{n \rightarrow \infty} \frac{1}{n} \sum_{t=1}^n Z_t \tag{3}$$

where  $Z_t = 1$  if  $X_t \in S$  and  $Z_t = 0$  if  $X_t \in F$ . Here  $F$  represents "Failure state" and  $n$  is the total number of time steps.

Resilience ( $R$ ) describes how quickly a system will recover from failure state once failure has occurred [Hashimoto et al., 1982]. It may be defined as the system's average recovery rate. Thus, it is given by

$$R = \frac{\rho}{1 - \alpha} \tag{4}$$

where  $\rho = P[X_t \in F, X_{t+1} \in S] = P[X_t \in S, X_{t+1} \in F]$ ,  $\alpha = P[X_t \in S]$ .

From a given series, resilience can be computed as

$$R = \frac{\lim_{n \rightarrow \infty} \frac{1}{n} \sum_{t=1}^n W_t}{1 - \left( \lim_{n \rightarrow \infty} \frac{1}{n} \sum_{t=1}^n Z_t \right)} \tag{5}$$

where  $W_t$  indicates the event of transformation "from satisfactory to failure state" (or vice versa).  $W_t = 1$  if  $X_t \in S$  and  $X_{t+1} \in F$  and  $W_t = 0$  otherwise.

The resilience can also be expressed as the conditional probability of recovery from failure state, i.e.,

$$R = P[X_{t+1} \in S | X_t \in F] \tag{6}$$

Vulnerability ( $V$ ) is a measure of the severity of damage caused by a failure event. Hashimoto et al. [1982] defined it as

$$V = \sum_{j \in F} s(j)e(j) \tag{7}$$

where  $s(j)$  is the numerical indicator of severity for an observation  $x(j)$ , which belongs to unsatisfactory state.  $e(j)$  is the probability of that  $x(j)$ , corresponding to  $s(j)$ , which is the most unsatisfactory and severe outcome that occurs from the set of unsatisfactory states.

In risk analysis of water supply systems, the water deficit is often taken as the severity of failure [Jinno et al., 1995]. Following this concept,  $s(j)$  of equation (7) is replaced with  $v(j)$  which is the deficit volume of soil moisture. In the absence of specific knowledge about the probability  $e(j)$  of occurrence of an event of severity  $s(j)$ , they are assumed to be equiprobable [Jinno et al., 1995]. Hence, a value of  $(\frac{1}{n})$  is assigned to  $e(j)$  in equation (7) to obtain the following simplified equation of vulnerability, which is equal to the mean deficit volume

$$V = \frac{1}{n} \sum_{j=1}^n v(j) \tag{8}$$

where  $v(j)$  is the deficit volume at the  $j$ th time step and  $n$  is the total number of time steps as mentioned before.

In the context of soil moisture, when it falls below the PWP, plant life is under stress and "failure" is said to occur, analogous to the failure of reservoir system. Thus, considering PWP as the threshold, the RRV

measures can be computed for soil moisture series using equations (3), (5), and (8). In order to obtain a reasonably stable estimate, Maity et al. [2013] showed that 5 year temporal scale is optimum (please refer to section 2.3 for details). Thus, the monthly soil moisture time series is segmented into 5 years moving window and a series of RRV estimates are obtained from monthly soil moisture series of 50 years. It may be reiterated that though the soil moisture time series exhibits seasonality at monthly scale, the RRV series are not expected to show such cyclicity resulting from annual seasonality since each value of RRV series represents a 5 year block. Second, reliability and resilience are expected to follow a deterministic relation as indicated in equation (4). However, both reliability/vulnerability and resilience/vulnerability exhibit a stochastic relationship. Thus, the joint relationship between any of these two pair will bear the signature of drought characteristic for a given region.

### 2.2. Joint Probability Distribution of Resilience and Vulnerability Using Copula

The joint probability distribution between resilience and vulnerability is developed. Copulas are established to be the best choice for modeling the joint distributions between marginals with dependence. It has been applied successfully in a number of hydrological analyses in recent times [Renard, 2011; Palynchuk and Guo, 2011; Zhang et al., 2011; Vandenberghe et al., 2011]. Most of the copulas are suitable for modeling joint distribution of positively correlated random variables, while some of them (Plackett, Gaussian, and Frank) can handle negatively associated random variables. As resilience and vulnerability are found to be negatively correlated, their joint distribution is modeled with Plackett copula, which is found to be more suitable, compared to other copulas like Frank and Gaussian with Gaussian as closest competitor [Maity et al., 2013]. The Plackett copula has been successfully applied in a number of hydrological analyses recently [Kao and Govindaraju, 2008; Song and Singh, 2010a, 2010b]. A brief mathematical background of copulas, in general, and of Plackett copula, in particular is given in Appendix A. In order to compute the spatial variation, joint probability distribution can be obtained separately for different regions having different PWP as threshold. This is explained further later in the context of the study domain having a wide range of PWP.

### 2.3. Computation of Drought Management Index (DMI)

An important issue in the design of DMI is the length of temporal scale to be considered. In order to obtain a stable index as well as the finest possible temporal resolution to assess the long-term variation of drought characteristics, the aim is to select the minimum possible length of temporal blocks from which a reasonably stable estimate of the index can be obtained. In an earlier study [Maity et al., 2013], a sensitivity analysis was carried out to investigate the possible impact of the length of temporal blocks on the DMI computation. Two year through 10 year blocks were considered separately for computing the intermediate measures (i.e., RRV) and then DMI for five different soil moisture series from a range of climatic types. It was observed in each case that the DMI variation was noisy with high frequency fluctuation at 2 year, 3 year, or even 4 year scales but the value stabilized beyond 5 year scale. Hence, 5 year blocks have been used in this study.

DMI [Maity et al., 2013] is designed such that it increases with *increase in vulnerability* as well as with *decrease in resilience* and vice versa. DMI is the joint probability of exceedence of resilience and non exceedence of vulnerability of a soil moisture series using the relevant PWP value. That is

$$DMI_{\tau}^{loc} = P[R > r_{\tau}^{loc}, V \leq v_{\tau}^{loc}] \quad (9)$$

where  $P[\otimes]$  stands for probability of the event  $[\otimes]$ .  $r_{\tau}^{loc}$  and  $v_{\tau}^{loc}$  are the specific values of reduced resilience and reduced vulnerability, respectively, for a given location, *loc*, and for a given 5 year period,  $\tau$ . Being a probabilistic measure, range of DMI is 0–1; higher the value, higher the drought propensity and vice versa. Over the successive periods of 5 year moving window, DMI values can be computed to get the series that bears the temporal variation. Similarly, over the different locations (preferably gridded) such series can be computed to obtain the spatiotemporal variation of DMI.

## 3. Study Area and Data

The mainland of India, lying between 8°4'N and 37°6'N latitudes and 68°7'E and 97°25'E longitudes, constitutes the study domain for illustration. Monthly gridded (0.5° lat × 0.5° long) soil moisture values (in mm), reconstructed by Fan and van den Dool [2004], are obtained from the Climate Prediction Centre (CPC), NOAA (<http://www.esrl.noaa.gov/psd/data/gridded/data.cpcsoil.html>) for the period 1961–2010 for this

analysis. As per the data provider, these soil moisture values are estimated by a one-layer leaky bucket model (van den Dool *et al.*, 2003) and the model parameters are constant spatially as it is tuned based on Oklahoma observed runoff data ([http://www.cpc.ncep.noaa.gov/soilmst/leaky\\_glb.htm](http://www.cpc.ncep.noaa.gov/soilmst/leaky_glb.htm)). In fact, these are assumed to be constant all over the world! It represents the water content in a single soil column of depth 1.6 m having a maximum water holding capacity of 760 mm and a common porosity of 0.47. It is obvious that in reality, all soils in India do not have a porosity of 0.47 or a water holding capacity of 760 mm. Rather, the amount of water contained in a soil column of depth that has “equivalent” water holding capacity of 760 mm has been considered.

As mentioned before, the PWP value at each location is used as a threshold, differentiating the success and failure stages. The PWP data, specific to the broad soil types in India were compiled by Rao [1997] based on field observations that were reported in earlier literatures. Using this, the PWP data at each of the GCM grid intersection points (where soil moisture data are available) over India are determined. It worthwhile to note here that the PWP values under field conditions are not constant for any given soil type but are determined by the integrated effects of plant, soil, and atmospheric conditions. However, PWP is normally defined as the water content of a soil when most plants (corn, wheat, and sunflowers) growing in that soil wilt and fail to recover their turgor upon rewetting. The PWP values, compiled by Rao [1997], are a constant (characteristic) of the soil and independent of environmental conditions. The matric potential at this soil moisture condition is estimated at  $-15$  bar.

## 4. Results and Discussions

### 4.1. PWP Across India

The compilation by Rao [1997] gives the range of PWP values for different soil types in India. Based on that, four different PWP values—10%, 25%, 17%, and 5% are considered as representative PWP values for the four broad soil types—alluvial, black, red & laterite, and desert soil, respectively. These four broad soil types constitute 82% of the total land area of India. Remaining 18% belong to the other soil types (e.g., mountain, saline, alkaline, and organic) for which limited information are available. Since specification of CPC soil moisture data suggests an equivalent depth of 1.6 m soil column, the PWP for alluvial, black, red & laterite, and desert soil are obtained as 160 mm, 400 mm, 272 mm, and 80 mm, respectively. Figure 1 illustrates a digitized gridwise PWP map of the study area. For each location (grid cell), RRV values are computed using the PWP value specific to the soil type at that location.

### 4.2. Computation of RRV Across India

The study period (1961–2010) is divided into 46 blocks of 5 year moving windows (1961–1965, 1966–1970, . . . , 2006–2010). Putting  $n = 60$  (corresponding to 60 months in a 5 year period) in equation (3), reliability is calculated for each of the 46 overlapping periods at each location. If the soil moisture does not fall below the threshold even once during the 5 year period, then reliability is obtained as 1 for that duration. Corresponding resilience values are considered as maximum, i.e., 1. For any other value of reliability, resilience is determined from equation (5), putting  $n = 60$ . Vulnerability is computed for each time segment using equation (8). The unit of vulnerability is mm, whereas reliability and resilience are unitless as they are measured on the probability scale, i.e., 0–1.

The spatiotemporal variations of RRV values across India during 1961–2010 are presented in the form of contour plots (Figures 2–4) for some typical time steps (successive 5 year periods, i.e., 1961–1965, 1966–1970, . . . , 2006–2010). For instance, Figure 2a displays reliability map for the period 1961–1965, Figure 2b displays reliability map for the period 1966–1970, and so on. Similarly, Figures 3a–3j present the resilience maps and Figures 4a–4j present the vulnerability maps. It is observed in most of the subplots of Figure 2 that reliability is quite high (between 0.7 and 1) toward the north and northeastern parts of India. However, the western part of peninsular India has low reliability (between 0 and 0.3) consistently for the past 50 years. Figure 3 indicates that resilience is rather low (less than 0.3) across the entire country except the Himalayan foothills in the north and north-east (around 0.8). The vulnerability contour maps (Figure 4) show that vulnerability is low (less than 25 mm) across the whole of northern and north-eastern India, but on the higher side (between 140 and 175 mm) toward the western part of peninsular India. It is observed that RRV maps have a correspondence to the soil type patterns but not necessarily always. When observed in detail, it is found that although reliability tends to be high in the alluvial soils having a relatively small PWP, it is rather

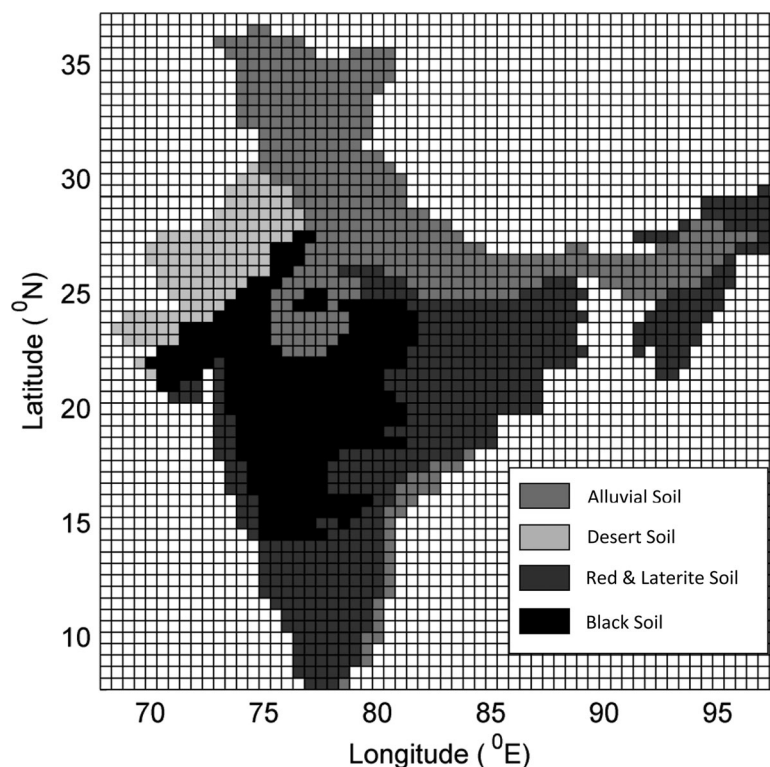


**Figure 1.** PWP map of India: Alluvial, black, red & laterite, and desert soil with PWP of 160 mm, 400 mm, 272 mm, and 80 mm, respectively.

low in the desert soils having even smaller PWP. Moreover, the measures are also found to vary slowly over time indicating a possible change in drought characteristics at many places. Thus, besides soil type, RRV are also expected to depend on a combination of various factors, such as, climate, land use, and land cover. The alluvial soils in India are mostly located in the regions of high rainfall, for example, the Gangetic plain in north India with annual average rainfall of about 100 cm. As water availability is high in these regions, the chances of soil moisture remaining below PWP are low. This explains the observation that alluvial soils (with small PWP) tend to have high reliability. On the other hand, the desert soil observed in the western part of the country in Rajasthan has very low PWP. The average annual rainfall varies from 31 cm in western Rajasthan to 67 cm in eastern Rajasthan. As water availability is very low, the soil moisture tends to remain below PWP and reliability is quite low.

The pairwise relationships of RRV for the period 1961–1996 are shown in Figures 5a and 5b. The four different markers in these scatter plots correspond to data from four different soil types. In Figure 5a, the number of data points seems to be much less than that in Figure 5b. This is because many of the data points are coincident in the reliability-resilience plot and thus cannot be spotted individually. At any given region, reliability and resilience of soil moisture series are related by a mathematical equation (equation (4)), hence, their relationship is deterministic in nature. Hashimoto *et al.* [1982] observed that the presence of a well-defined deterministic relationship between reliability and resilience allows the quantification of one given the other. Moreover, the scatter plot (Figure 5a) also indicates the monotonic behavior of reliability and resilience. Hence, as mentioned in methodology, either of reliability and resilience can be used along with vulnerability for probabilistic assessment of drought propensity through DMI. Toward this, spatiotemporal variation of DMI over the study region using resilience and vulnerability is discussed in the following subsections.

#### 4.3. Computation and Spatiotemporal Variation of DMI

The resilience and vulnerability are found to be negatively correlated. Thus, their joint distribution is modeled with Plackett copula as discussed in the methodology. First, all the grid locations over India are

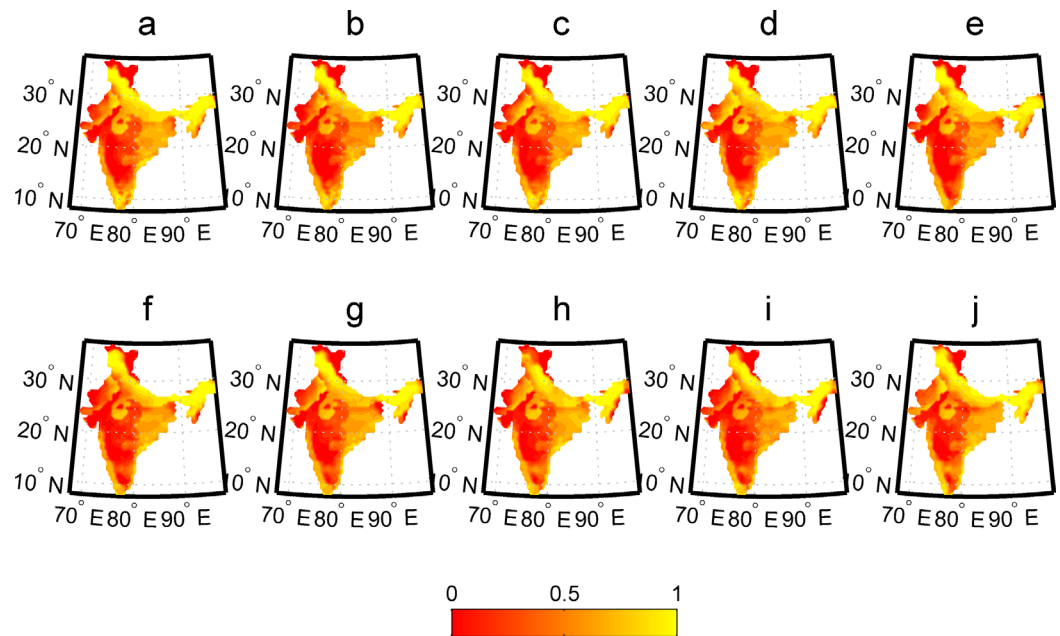


**Figure 2.** Spatiotemporal variations of reliability across India during (a) 1961–1965, (b) 1966–1970, (c) 1971–1975, (d) 1976–1980, (e) 1981–1985, (f) 1986–1990, (g) 1991–1995, (h) 1996–2000, (i) 2001–2005, and (j) 2006–2010.

grouped into four categories based on the soil type, such that the resilience and vulnerability series for the development period at all the locations for a given soil type are pooled together to develop the copula parameters. For alluvial, black, red & laterite, and desert soil, the dependence parameters are obtained as  $\theta_1=0.0263$ ,  $\theta_2=0.0318$ ,  $\theta_3=0.0487$ , and  $\theta_4=0.0249$ , respectively. Four joint CDFs of resilience and vulnerability are computed using the copula parameters of the respective soil type. Subsequently, DMI is computed at each time step (starting from 1961 to 1965, 1962 to 1966 through 2006 to 2010) and at each location using equation (9) from the corresponding joint CDF, specific for that region. The

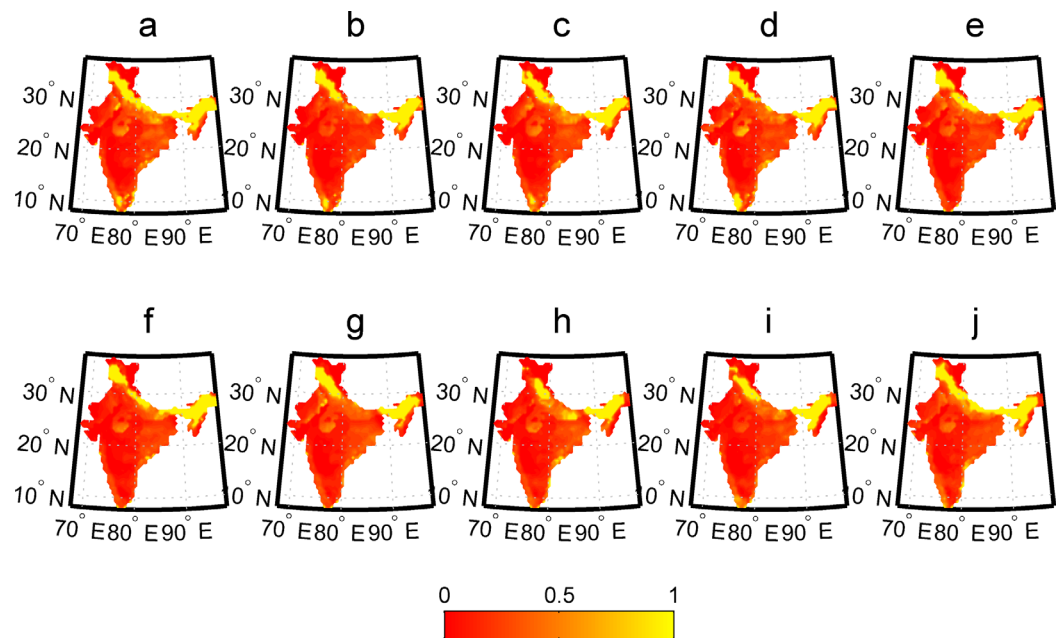


**Figure 3.** Spatiotemporal variations of resilience across India during (a) 1961–1965, (b) 1966–1970, (c) 1971–1975, (d) 1976–1980, (e) 1981–1985, (f) 1986–1990, (g) 1991–1995, (h) 1996–2000, (i) 2001–2005, and (j) 2006–2010.

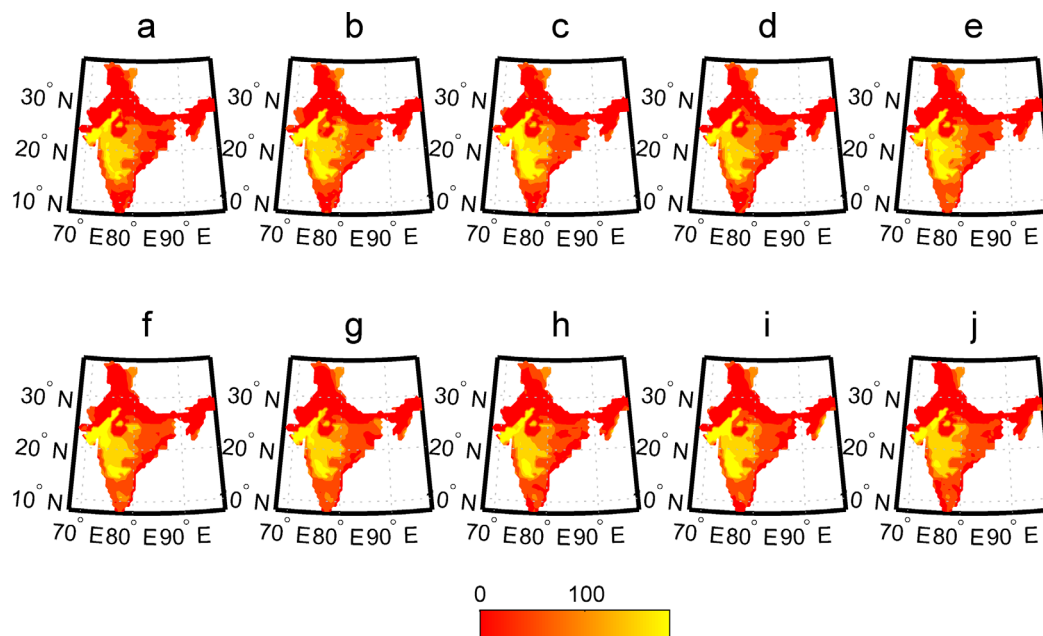


**Figure 4.** Spatiotemporal variations of vulnerability across India during (a) 1961–1965, (b) 1966–1970, (c) 1971–1975, (d) 1976–1980, (e) 1981–1985, (f) 1986–1990, (g) 1991–1995, (h) 1996–2000, (i) 2001–2005, and (j) 2006–2010.

spatiotemporal variation of DMI can be shown by a series of DMI contour plots. A series of such contour plots of DMI across the study region is shown in Figure 6 for some selected time steps (successive 5 year periods, i.e., 1961–1965, 1966–1970, . . . , 2006–2010). From Figure 6, spatial variation is clearly visible. DMI is found to be consistently low in north east India. It is also low in central India and the northern foothills. In the western tip and in the peninsular India, DMI is found to be comparatively high, indicating higher drought propensity. Temporal variation is also apparent from the series of these plots. In the context of such spatiotemporal variation of DMI, its utility and predictability are discussed in the subsequent sections.

#### 4.4. Utility of DMI

This section illustrates, that DMI, which incorporates the resilience and vulnerability of the system, is better at characterizing the drought characteristics rather than using a single metric. The amount by which the soil moisture deviates from the minimum level required for crop growth (represented by PWP of the region) is captured successfully by the DMI in situations where reliability fails to make a distinction. Let us consider two locations A and B (refer Figure 7a) within same soil type (alluvial). During 1961–1965, these locations have identical values of reliability (0.95) and significantly different values of DMI (0.255 and 0.606, respectively). The DMI values reflect the considerable difference in soil moisture deficit (31.6 mm and 146.1 mm, respectively). Higher DMI, indicating higher drought propensity, corresponds to more serious droughts marked by higher shortfalls in soil moisture at those locations. Similar behavior is observed at other time steps as well. Thus, even if the reliability of soil moisture is same for two locations at a given point in time, they may be exposed to different magnitudes of drought propensities—as represented by their DMI. As a result, they may require separate strategies in terms of drought preparedness, crop planning, and water allocation. At any particular location, in general, if the soil moisture deficit falls between two time steps, it results in a decrease in DMI. For example, at location C (refer Figure 7a) in red & laterite soil, the DMI is found to fall slightly (from 0.285 to 0.277) during 1961–1965 to 1966–1970. This is the results of a drop in soil moisture deficit from 2481 mm to 2064 mm.

Whereas the aforementioned examples are straightforward, the aim of developing spatiotemporal variation of DMI is to characterize the drought propensity of a region considering both the average deficit when a drought has occurred (vulnerability) and the chance of recovery (resilience). Thus, a simple rise (or drop) in

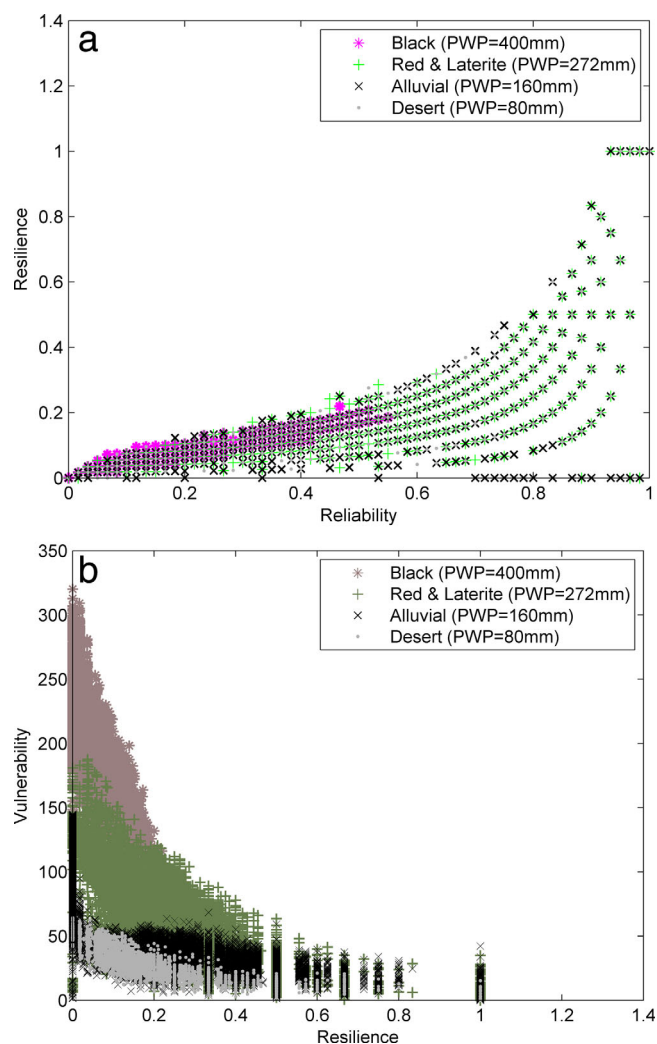


**Figure 5.** (a) Scatter plot between reliability and resilience. (b) Scatter plot between resilience and vulnerability.

48.7 mm during 1961–1965). Consequently, DMI is lower during 1966–1970 indicating fall in drought propensity.

#### 4.5. Predictability of DMI

Predictability of any drought index helps in adapting drought management policies in near future. In general, the predictability of most of the existing drought indices is a challenging issue. Hence, it is particularly interesting to explore the predictability of the recently developed drought index DMI using its endogenous property for a particular location. DMI, being a long-term (5 year time scale) drought index, its predictability can be effectively used in long-term drought management and preparedness. It will further help in assessing the future drought propensity for a particular location/region even though the future soil moisture data are not known.

The temporal variation of DMI at a few locations within each soil type is investigated. The past behavior of in DMI, if modeled suitably, can be used to estimate near-future (at least next 5 year period) drought propensity at a region. A model is developed here to explore the predictability of DMI. The period 1961–1996 is taken as the development period and 1993–2010 is taken as testing period for this model.

Since DMI is a probabilistic index, it ranges from 0 to 1. For proper modeling, the observed DMI series of each location is mapped onto the real line by employing the inverse CDF of a standard Gaussian

soil moisture deficit does not necessarily indicate a higher (or lower) drought propensity, which should reflect from the DMI values. In other words, rise (or drop) in soil moisture deficit is not necessarily always accompanied by a rise (or drop) in DMI. Let us consider location B where DMI drops (0.606–0.408) between 1961–1965 and 1966–1970 in spite of an increase (146.1–285.2 mm) in cumulative soil moisture deficit over this period. This may be counter intuitive at first but a look at the soil moisture time series (Figure 7b) during the concerned period explains the apparent paradox. During the period 1961–1965, the soil moisture falls below the threshold only once. However, during 1966–1970, the soil moisture falls below the threshold 5 times and rebounds each time within a reasonable period. Thus, it is possibly characterized by quick recovery from dry spells as it has an improved recovery record. Hence, it attains a higher value of resilience, i.e., 0.416 compared to 0.333 in the previous time step. Moreover, very small deficits in some of the five failure events during 1966–1970 pull down the average deficit resulting in a lower value of vulnerability (23.7 mm during 1966–1970 as opposed to

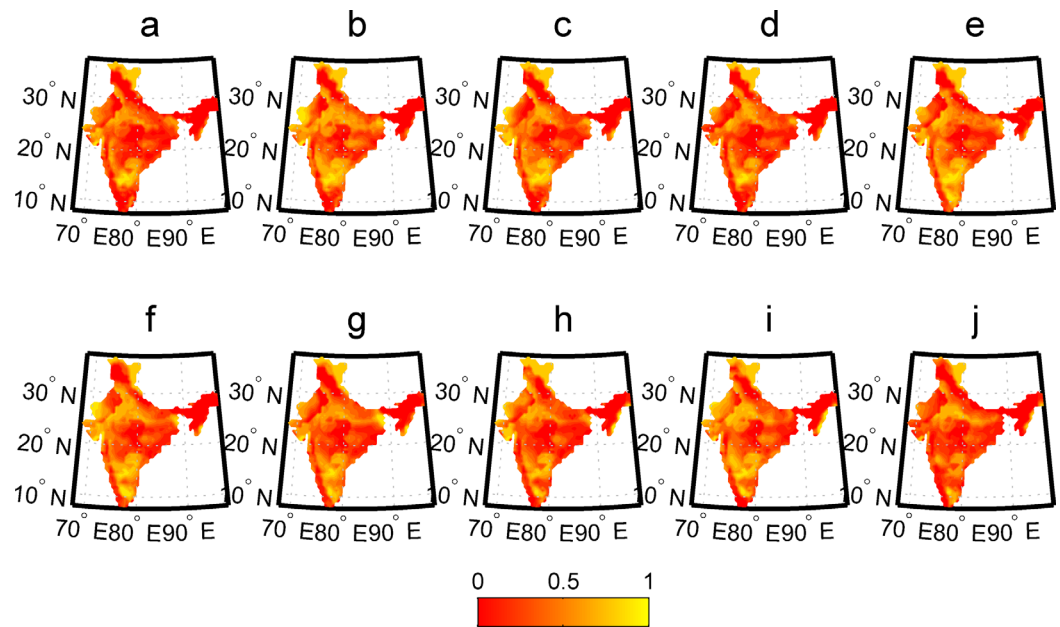


**Figure 6.** Spatiotemporal variations of DMI across India during (a) 1961–1965, (b) 1966–1970, (c) 1971–1975, (d) 1976–1980, (e) 1981–1985, (f) 1986–1990, (g) 1991–1995, (h) 1996–2000, (i) 2001–2005, and (j) 2006–2010.

distribution. These transformed series have been subsequently modeled using a deterministic and a stochastic component. The modeled values, obtained by summing the components, are back transformed to get the required DMI series in the probability scale for comparison with the observed DMI series. It may be noted here that while transforming the DMI from the probability scale to the real line, the DMI values 0 and 1 will be transformed to  $-\infty$  and  $\infty$ , respectively. If undefined values are present in a series, neither a deterministic model nor a stochastic model can be fitted to it to obtain any useful information. This issue has been handled by replacing  $-\infty$  with  $-3$ , and  $\infty$  with  $3$  in the transformed series. This step can be justified by the fact that 99.73% of the values lie between  $-3$  and  $3$  in a standard normal distribution. It is worthwhile to mention here that numerous combinations of mean and standard deviation of the normal distribution are considered before zeroing in on the standard normal distribution for non linear mapping of DMI. It is observed that the best prediction performance (in terms of the spatially averaged performance measures as well as the spatial uniformity of gridwise performances) is obtained in case of standard normal distribution, i.e.,  $N(0,1)$ .

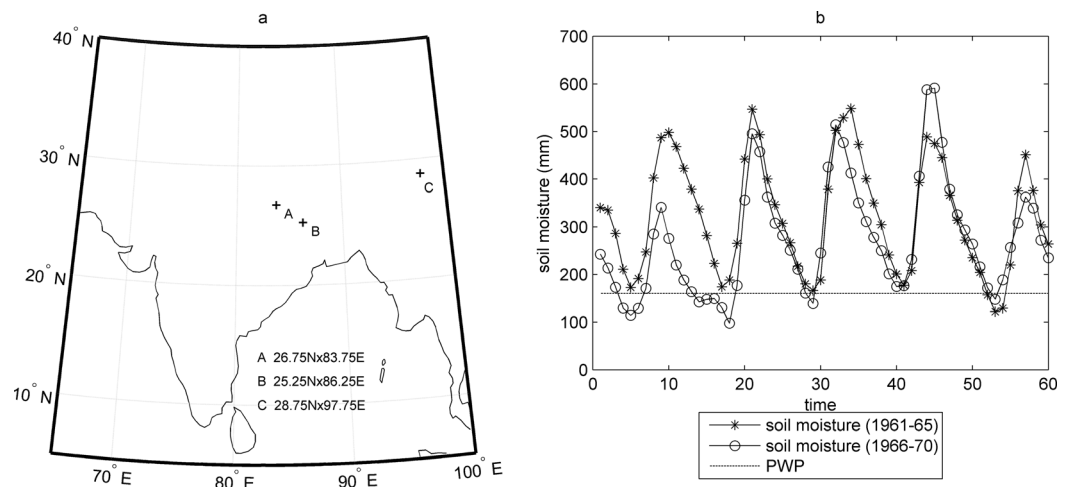


**Figure 7.** (a) Sample locations (with latitude and longitude) having same reliability and different DMI, (b) soil moisture series during 1961–1965 and 1966–1970 at location B.

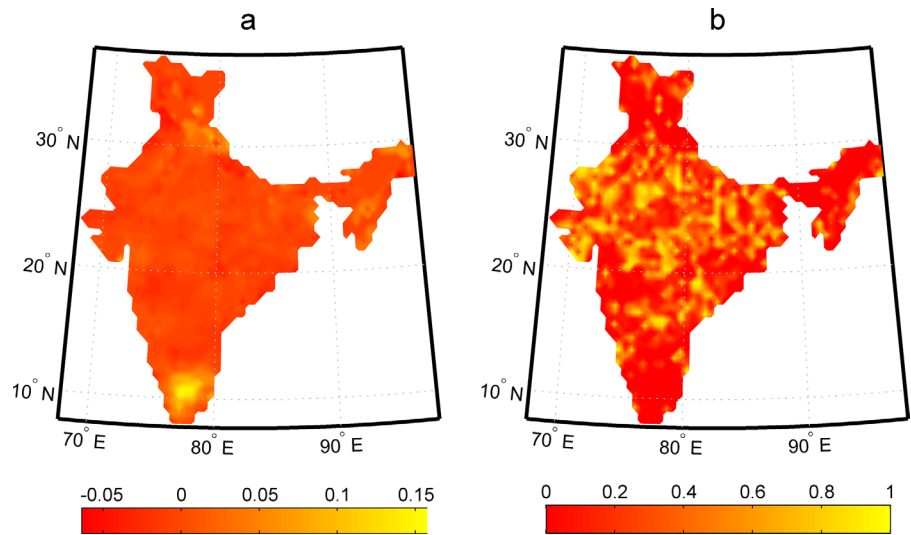


**Figure 8.** Spatial variation of (a) slope of the linear trend of DMI and (b)  $p$ -value of the linear trend.  $p$ -values at 507 locations are found to be significant at 95% confidence level (below 0.05).

Out of 1267 grid locations in India, linear trend of DMI variation is significant (at 5% level of significance) at 507 locations. Figure 8 shows the spatial variation of the linear DMI trend and the  $p$ -value of the slope across India. The trend must be included in the prediction model for the locations where it is significant. Even for those locations where it is not significant, the linear component is still included in the model because any deterministic component, however small, should be extracted first before applying stochastic model to the residuals. Obviously, the inclusion of trend would not affect adversely the performance of the model. The DMI series indicate the presence of periodicity at 548 out of the 1267 grid locations in India. For the remaining locations, the periodic subcomponent is excluded since the periodicity is absent. Thus, the deterministic component of DMI series is captured via two subcomponents—linear trend and periodicity. The Box-Jenkins approach is used to model the stochastic component. After an initial investigation of the autocorrelogram and partial autocorrelogram, an AR(1) model is found to be the most suitable for modeling the residuals. Thus, the modeled DMI is given by

$$y_{m,\tau} = y_{1,\tau} + y_{2,\tau} + y_{3,\tau} \quad (10)$$

where  $y_1$ ,  $y_2$ , and  $y_3$  represent the linear trend component, periodic component, and the stochastic component, respectively, and  $\tau$  is the time step referring to the successive moving 5 year periods from 1961 to 1996, i.e., 1961–1965, 1962–1966, . . . , 1992–1996 over which DMI are calculated. The  $y_1$  is given by

$$y_{1,\tau} = p_1\tau + p_2 \quad (11)$$

where  $p_1$  and  $p_2$  are the linear trend parameters determined separately for each grid location. The parameter  $p_1$  is found to range from 0.16 to  $-0.06$ , while  $p_2$  is found to range from 1.99 to  $-4.17$ .

The  $y_2$  is given by

$$y_{2,\tau} = a \cos \left( 2\pi \frac{\tau}{T} + \phi \right) \quad (12)$$

where  $a$  is the amplitude ranging from 1.388 to 0.0064,  $T$  is the time period of the detrended series at the concerned grid location and it ranges from 2.03 to 15.95 time steps.  $\phi$  is the phase angle ranging from  $359.99^\circ$  to  $0.01^\circ$  with 136 locations having a phase angle of less than  $1^\circ$ .

The AR(1) model for the residuals is expressed as

$$Y_{3,\tau} = b \times Y_{3,\tau-1} + e_\tau \quad (13)$$

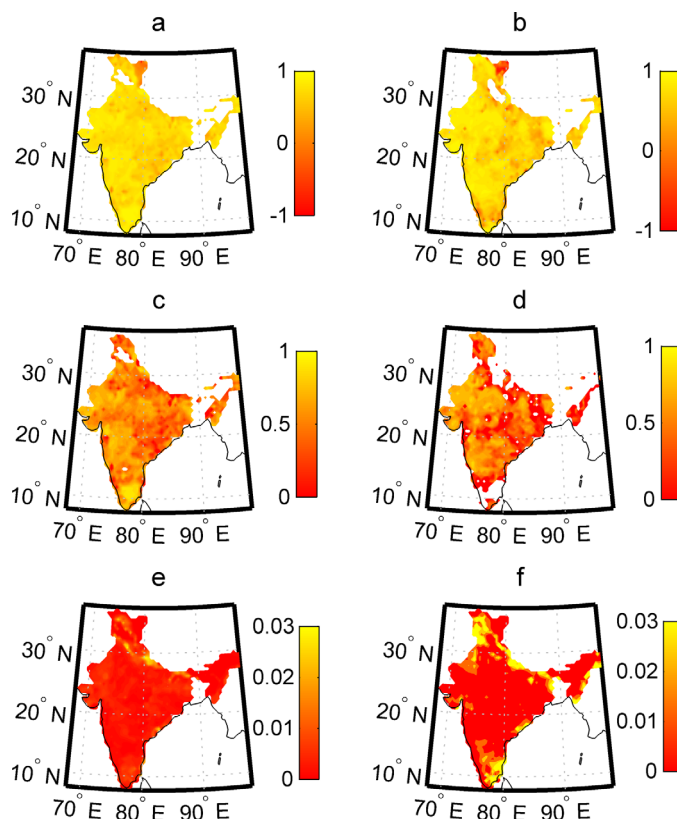


**Figure 9.** Spatial variation of model performance. Contour plot of Pearson correlation coefficient between modeled and computed DMI for the (a) model development and (b) testing period. Nash Sutcliffe Efficiency (NSE) of modeled DMI during (c) model development and (d) testing period. Mean Squared Error (MSE) of modeled DMI during (e) model development and (f) testing period. Correlation could not be calculated in the north eastern region as DMI is constant. NSE is reasonably good over many, if not most, parts of the country. The blank portions correspond to regions where NSE is negative, so that the predictive capacity of the model is nil in those regions.

for the model development period and testing period in Figures 9e and 9f, respectively. Except for a few locations, the NSE is found to be mostly positive (ranging from 0.1 to 0.9). In brief, the prediction model is applicable over most of the study area and its performance is more or less uniform spatially. However, for certain regions, such as the eastern part of Kashmir, the correlation coefficient between modeled and observed DMI is close to zero and the NSE is negative. This is perhaps due to the fact that observed DMI values are almost constant in these locations, lying between 0.87 and 0.88. Though the predicted DMI values are also similarly high (lying mostly between 0.86 and 0.89), leading to very low MSE of the model in these locations (Figures 9e and 9f), the NSE values are negative, since the predicted values do not reflect the observed values any better than the mean values. Similar cases are also noticed in the southern parts of Jammu & Kashmir and parts of Assam. The DMI series is constant in these zones and thus correlation coefficient could not be calculated and NSE is also negative due to the reason mentioned earlier. Still, the MSE values are very low, comparable to that in the rest of the study area (Figure 9). Thus, it may be stated that the performance measures indicate a reasonably good predictability of DMI at many, if not most, locations that can be effectively used in drought management and preparedness.

Thus, the possibility of an early prediction of DMI provides catchment managers some advance information regarding what to expect over the next 5 years at any given region. If a region is found to dry up gradually, then adaptive measures may be taken such as replacement of traditionally grown crops with less water intensive crops. If DMI prediction is made sufficiently early, increased irrigation network may also be established.

Before concluding, it may be mentioned that the underlying assumption of RRV computation is that the soil moisture is in *satisfactory* state if it is above the PWP, with no annotation as to *how much* above PWP. In

where  $b$  is the coefficient of the AR(1) model fitted to the residuals,  $Y_3$ , and  $e_\tau$  is the error at the  $\tau$ th time step. Since the error  $e_\tau$  is assumed to be normally distributed with a mean 0 and standard deviation  $\sigma_{e_\tau}$ , the expected value of  $Y_3$ , i.e.,  $E(Y_3)$ , denoted as  $y_3$  can be expressed as

$$y_{3,\tau} = b \times y_{3,\tau-1} \quad (14)$$

The values of  $b$  are found to range from  $-0.16$  to  $0.96$ .

The Pearson correlation coefficient between the modeled and observed (i.e., computed from RRV) DMI at each grid location for the model development period and testing period are calculated and plotted in a contour map in Figures 9a and 9b, respectively. It is found to be above 0.6 over most of the study area. The Nash Sutcliffe Efficiency (NSE) of the modeled DMI is also computed and plotted for the model development period and testing period in Figures 9c and 9d, respectively. Similarly, the Mean Squared Error (MSE) of the modeled DMI is also computed and plotted

reality, even if the soil moisture depth is always above PWP, it may be harmful for crop growth as in the case of water logged areas. DMI is defined in such a manner that a location having a historical soil moisture series which never drops below PWP will have  $DMI=0$ , RRV values being 1, 1, and 0, respectively. This is a favorable case; however, it is not distinguishable from water logged areas, which are not favorable. Moreover, computation of DMI, based on RRV rationale, requires a threshold indicative of transition into water stress. PWP of four broad soil types in India are used in this study. If PWP at a finer resolution (preferably at the resolution of the soil moisture data set) is available, it would enhance the accuracy of the results. Finally, it is also worthwhile to mention another issue on the historical data length. In the study, 35 years data are used to demonstrate the temporal variation of DMI. Since it is expected that the nature of the DMI variation may alter in the long term due to change in land use and hydrological processes, this model is meant for near-term future prediction. Hence, for prediction of DMI over a certain period, the model development period should be defined such that the behavior of DMI in the most recent decades is incorporated in the prediction model. Thus, a moving window of 40–50 years immediately preceding the prediction period is ideal, in case longer data set is available.

## 5. Summary and Conclusions

This study introduces the scope of Drought Management Index (DMI), developed using RRV rationale, in assessing the spatiotemporal variation of drought propensity. Entire India, where soil type and PWP vary from one location to another, is considered as a study domain to establish that unlike traditional drought measures, which characterize the ongoing drought status using a single metric, DMI quantifies the drought propensity of a region using the joint behavior of resilience and vulnerability of soil moisture series. It is illustrated in this study that, DMI is able to categorically identify regions, which demand more attention in terms of drought management, even when soil moisture reliability fails to make a distinction. Gridwise quantification of drought propensity through DMI is particularly useful in monitoring the slowly varying drought characteristics for a location. The status of DMI over the past 50 years (1961–1965 to 2006–2010) indicate that drought propensity is consistently low toward northern and north eastern parts of India, but much higher in the western part of peninsular India. A model consisting of deterministic and stochastic components is developed to explore the predictability of DMI. The predictability of DMI for a lead time of 5 years is found to vary across India and the future estimates of DMI values are found to be reasonably good at most of the regions. This can be effectively utilized for better management and drought preparedness. On estimating the nature of DMI variation at a location, modifications in cropping practices and water allocation between competing river basins may be planned wisely. The concept behind DMI computation being general, the methodology can be extended to other hydrologic variables as well.

## Appendix A: Copula

A copula is a function that joins or couples together univariate marginal distributions to form a multivariate joint distribution [Nelsen, 2006]. Sklar's theorem [Sklar, 1959] is central to the concept of copulas. It states that for a joint distribution function  $H$  with margins  $F$  and  $G$ , there exists a copula  $C$  for all  $(x, y)$  in the extended real line  $\bar{R}$  such that

$$H(x, y) = C(F(x), G(y)) \tag{A1}$$

Thus, copula relates a multivariate distribution function to a lower dimensional marginal distributional function. In equation (A1), if  $F$  and  $G$  are continuous, then  $C$  is unique; also  $C$  is unique on simultaneous range of  $F$  and  $G$ . In the present study,  $X$  and  $Y$  resilience and vulnerability, respectively, and  $H$  is the joint distribution determined with Plackett copula, which is explained in the following subsection.

### A1. Plackett Copula

Plackett copula can model both positive and negative dependence between random variables. It has only one parameter and the copula can be constructed by using the algebraic relationship between the joint distribution function and its univariate margins. The bivariate Plackett copula [Plackett, 1965], which is used here to model the joint distribution of resilience and vulnerability is given by

$$C_p(u, v) = \frac{[1 + (\theta_p - 1)(u + v)] - \sqrt{[1 + (\theta_p - 1)(u + v)]^2 - 4uv\theta_p(\theta_p - 1)}}{2(\theta_p - 1)} \quad (\text{A2})$$

where  $u$  and  $v$  are the univariate marginals of resilience and vulnerability, respectively, and  $\theta_p$  is the dependence parameter, which is the cross product ratio between the random variables.  $\theta_p$  can be estimated by the pseudo likelihood function [Genest *et al.*, 1995] and can also be estimated directly from the observations and sample medians [Mardia, 1970]. The sample medians divide the observations into four quadrants: first, where observations of both resilience and vulnerability are greater than their respective median values, second, where observations are less than the median for resilience and greater than the median for vulnerability, third, where observations of both resilience and vulnerability are less than their respective median values, and fourth, where observations are greater than the median for resilience and less than the median for vulnerability. If  $\hat{\theta}_p$  is the cross product ratio estimated from observations, then it can be expressed as the following equation

$$\hat{\theta}_p = \frac{n_{00}n_{11}}{n_{01}n_{10}} \quad (\text{A3})$$

where  $n_{11}$ ,  $n_{01}$ ,  $n_{00}$ , and  $n_{10}$  are the number of observations in the first, second, third, and fourth quadrant, respectively. Possible range of  $\hat{\theta}_p$  is between zero to infinity. A value less than one indicates a negative association whereas positive association is indicated by the values greater than or equal to one.

#### Acknowledgments

We acknowledge the constructive suggestions of three anonymous reviewers that have helped to improve the manuscript substantially. We also acknowledge the partial financial support from the projects, sponsored projects by the Australia India Strategic Research Fund (AISRF) (Ref. No. DST/INT/AUS/P-27/2009) and Ministry of Earth Sciences (MoES) (Ref. No. MoES/PAMC/H&C/30/2013-PC-II). We further acknowledge that the monthly gridded ( $0.5^\circ \text{ lat} \times 0.5^\circ \text{ long}$ ) soil moisture values (in mm) is obtained from the Climate Prediction Centre (CPC), NOAA (<http://www.esrl.noaa.gov/psd/data/gridded/data.cpcsoil.html>).

#### References

- Bergman, K. H., P. Sabol, and D. Miskus (1988), Experimental indices for monitoring global drought conditions, in *Proceedings of the 13th Annual Climate Diagnostics Workshop*, pp. 190–197, U.S. Dep. of Commer., Cambridge, Mass.
- Bhalme, H. N., and D. A. Mooley (1980), Large-scale droughts/floods and monsoon circulation, *Mon. Weather Rev.*, *108*, 1197–1211.
- Blumenstock, G., Jr. (1942), Drought in the United States analyzed by means of the theory of probability, *Tech. Bull.* 819, U.S. Dep. Agric., Washington, D. C.
- Byun, H. R., and D. A. Wilhite (1999), Objective quantification of drought severity and duration, *J. Clim.*, *12*, 2747–2756.
- Dracup, J. A., K. S. Lee, and E. G. Paulson Jr. (1980), On the definition of droughts, *Water Resour. Res.*, *16*, 297–302.
- Fan, Y., and H. van den Dool (2004), Climate Prediction Center global monthly soil moisture data set at 0.5 degree resolution for 1948 to present, *J. Geophys. Res.*, *109*, D10102, doi:10.1029/2003JD004345.
- Genest, C., K. Ghoudi, and L.-P. Rivest (1995), A semiparametric estimation procedure of dependence parameter in multivariate families of distributions, *Biometrika*, *82*, 543–552.
- Hashimoto, T., J. R. Stedinger, and D. P. Loucks (1982), Reliability, resiliency, and vulnerability criteria for water resource system performance evaluation, *Water Resour. Res.*, *18*(1), 14–20, doi:10.1029/WR018i001p00014.
- Heim, R. R., Jr. (2002), A review of twentieth-century drought indices used in the United States, *Bull. Am. Meteorol. Soc.*, *83*, 1149–1165.
- Huang, J., H. van den Dool, and K. P. Georgakakos (1996), Analysis of model-calculated soil moisture over the United States (1931–93) and application to long-range temperature forecasts, *J. Clim.*, *9*, 1350–1362.
- Jinno, K., X. Zongxue, A. Kawamura, and K. Tajiri (1995), Risk assessment of a water supply system during drought, *Water Resour. Dev.*, *11*(2), 185–204.
- Kao, S.-C., and R. S. Govindaraju (2008), Trivariate statistical analysis of extreme rainfall events via the Plackett family of copulas, *Water Resour. Res.*, *44*, W02415, doi:10.1029/2007WR006261.
- Kao, S.-C., and R. S. Govindaraju (2010), A copula-based joint deficit index for droughts, *J. Hydrol.*, *380*(1–2), 121–134.
- Keyantash, J., and J. A. Dracup (2002), The quantification of drought: An evaluation of drought indices, *Bull. Am. Meteorol. Soc.*, *83*, 1167–1180.
- Kogan, F. N. (1995), Droughts of the late 1980s in the United States as derived from NOAA polar-orbiting satellite data, *Bull. Am. Meteorol. Soc.*, *76*(5), 655–668.
- Kogan, F. N. (1997), Global drought watch from space, *Bull. Am. Meteorol. Soc.*, *78*, 621–636.
- Liu, W. T., and F. N. Kogan (1996), Monitoring regional drought using the vegetation condition index, *Int. J. Remote Sens.*, *17*, 2761–2782.
- Maitly, R., A. Sharma, D. N. Kumar, and K. Chanda (2013), Characterizing drought using the reliability-resilience-vulnerability concept, *J. Hydrol. Eng.*, *18*(7), 859–869, doi:10.1061/(ASCE)HE.1943-5584.0000639.
- Mallya, G., S. Tripathi, S. Kirshner, and R. S. Govindaraju (2013), Probabilistic assessment of drought characteristics using hidden Markov model, *J. Hydrol. Eng.*, *18*(7), 834–845, doi:10.1061/(ASCE)HE.1943-5584.0000699.
- Mardia, K. V. (1970), *Families of Bivariate Distributions*, Griffin, London, U. K.
- McGuire, J. K., and W. C. Palmer (1957), The 1957 drought in the eastern United States, *Mon. Weather Rev.*, *85*, 305–314.
- McKee, T. B., N. J., Doesken, and J. Kleist (1993), The relationship of drought frequency and duration to time scales, paper presented at Eighth Conference on Applied Climatology, American Meteorological Society, Calif.
- McQuigg, J. (1954), A simple index of drought conditions, *Weatherwise*, *7*, 64–67.
- Modarres, R. (2007), Streamflow drought time series forecasting, *Stochastic Environ. Res. Risk Assess.*, *21*(3), 223–233.
- Munger, T. T. (1916), Graphic method of representing and comparing drought intensities, *Mon. Weather Rev.*, *44*, 642–643.
- Nelsen, R. B. (2006), *An Introduction to Copulas*, Springer, N. Y.
- Palmer, W. C. (1965), Meteorological drought. Res. Paper No. 45, 768 Weather Bureau, Washington, D. C.
- Palmer, W. C. (1968), Keeping track of crop moisture conditions, nationwide: The new crop moisture index, *Weatherwise*, *21*, 156–161.
- Palynchuk, B. A., and Y. Guo (2011), A probabilistic description of rain storms incorporating peak intensities, *J. Hydrol.*, *409*(1–2), 71–80.

- Panu, U. S., and T. C. Sharma (2002), Challenges in drought research: Some perspectives and future directions, *Hydrol. Sci. J.*, 47(1), S19–S30, doi:10.1080/02626660209493019.
- Plackett, R. L. (1965), A class of bivariate distributions, *J. Am. Stat. Assoc.*, 60, 516–522.
- Rao, N. H. (1997), Grouping water storage properties of Indian soils for soil water balance model applications, *Agric. Water Manage.*, 36, 99–109.
- Renard, B. (2011), A Bayesian hierarchical approach to regional frequency analysis, *Water Resour. Res.*, 47, W11513, doi:10.1029/2010WR010089.
- Shafer, B. A., and L. E. Dezman (1982), Development of a Surface Water Supply Index (SWSI) to assess the severity of drought conditions in snowpack runoff areas, in *Preprints, Western Snow Conference*, pp. 164–175, Colo. State Univ., Reno, Nev.
- Sivakumar, M. V. K., and D. A. Wilhite (2002), Drought preparedness and drought management, paper presented at International Conference on Drought.
- Sklar, A. (1959), Fonctions de répartition à n dimensions et leurs marges, *Publ. l'Inst. Stat. l'Univ. Paris*, 8, 229–231.
- Song, S., and V. P. Singh (2010a), Frequency analysis of droughts using the Plackett copula and parameter estimation by genetic algorithm, *Stochastic Environ. Res. Risk Assess.*, 24(5), 783–805, doi:10.1007/s00477-010-0364-5.
- Song, S., and V. P. Singh (2010b), Meta-elliptical copulas for drought frequency analysis of periodic hydrologic data, *Stochastic Environ. Res. Risk Assess.*, 24(3), 425–444, doi:10.1007/s00477-009-0331-1.
- Thornthwaite, C. W. (1931), The climate of North America according to a new classification, *Geogr. Rev.*, 21, 633–655.
- van den Dool, H., J. Huang, and Y. Fan (2003), Performance and analysis of the constructed analogue method applied to US soil moisture applied over 1981–2001, *J. Geophys. Res.*, 108(D16), 8617, doi:10.1029/2002JD003114.
- van Rooy, M. P. (1965), A rainfall anomaly index independent of time and space, *Notos*, 14, 43.
- Vandenberghe, S., N. E. C. Verhoest, C. Onof, and B. De Baets (2011), A comparative copula-based bivariate frequency analysis of observed and simulated storm events: A case study on Bartlett-Lewis modeled rainfall, *Water Resour. Res.*, 47, W07529, doi:10.1029/2009WR008388.
- Waggoner, M. L., and T. J. O'Connell (1956), Antecedent precipitation index, *Weekly Weather Crop Bull.*, XLIII, 6–7.
- Yuan, X., and E. F. Wood (2013), Multimodel seasonal forecasting of global drought onset, *Geophys. Res. Lett.*, 40, 4900–4905, doi:10.1002/grl.50949.
- Zhang, Q., Chen, Y., Chen, X., and J. Li (2011), Copula-based analysis of hydrological extremes and implications of hydrological behaviors in the Pearl River Basin, China, *J. Hydrol. Eng.*, 16(7), 598–607.